Complex Systems **5** (1991) 89–100

Numerical Simulations of Fluid Dynamics with a Pair Interaction Automaton in Two Dimensions

D. A. Wolf-Gladrow
Alfred Wegener Institute for Polar and Marine Research,
D-2850 Bremerhaven, Federal Republic of Germany

R. Nasilowski
Universität Oldenburg, FB Physik,
D-2900 Oldenburg, Federal Republic of Germany

A. Vogeler
Alfred Wegener Institute for Polar and Marine Research,
D-2850 Bremerhaven, Federal Republic of Germany

Abstract. We perform numerical experiments with a novel cellular-automaton fluid model. The model has simple pair-interaction rules and works in arbitrarily many dimensions; here we consider the two-dimensional case. By observing the smoothing-out of the velocity profile of a shear flow and the relaxation of a shear wave, we measure the kinematic shear viscosity and obtain a value of ≈ 0.5. To demonstrate the fluid-like behavior of our automaton model, we also simulate a flow past an obstacle (von Karman vortex street).

1. Introduction

A first attempt to simulate fluid dynamics by cellular automata was made by Hardy, de Pazzis, and Pomeau [6]. They invented a fully discrete two-dimensional lattice gas model on a square lattice with built-in conservation laws for mass (particle number) and momentum. The HPP model behaves qualitatively like a fluid, but cannot quantitatively simulate interesting fluid dynamical phenomena because of anisotropies in the hydrodynamics of the lattice gas. The possibility of quantitative fluid-dynamic simulation, however, has recently become available with the hexagonal lattice gas model by Frisch, Hasslacher, and Pomeau [4] in two dimensions, and the pseudo-four-dimensional face-centered hypercubic (FCHC) lattice gas model by d'Humières and Lallemand [3] in three dimensions. The hydrodynamics of these models, although anisotropic, can be shown by symmetry arguments to be quasi-isotropic in the sense that the hydrodynamics in the low-velocity

incompressible limit becomes isotropic and is equivalent to the usual incompressible Navier-Stokes dynamics [5].

Particularly the two-dimensional FHP model and variants thereof have been successfully applied to problems like porous media flow [14], solids in suspension [9], surface tension [1], immiscible fluids [16], autocatalytic reactions [2], and flame propagation [2]. Three-dimensional simulations using the FCHC model, however, are much more difficult, not only because of the three-dimensional space, but also because the rules of the FCHC model are very hard to formulate as an algorithm that should be relatively simple and computationally effective at the same time [7, 17].

These difficulties with the FCHC model in three dimensions, and also the awkward hexagonal geometry of the FHP model in two dimensions, can possibly be overcome by a new model that has recently been proposed by Ralf Nasilowski [12, 13]. The new model works in arbitrarily many dimensions on orthogonal lattices and has simple, deterministic rules with pair interactions between cells. Nevertheless, the hydrodynamics of this lattice gas model can be shown to be equivalent to the usual (isotropic) Euler equations in the low-velocity incompressible nondissipative limit, so it is in a certain sense quasi-isotropic. Theoretical results for the practically interesting dissipation transport coefficients, particularly the shear viscosity, have not yet been obtained.

In this article, we present first results of computer experiments that have been performed with the two-dimensional version of the new automaton model. In the first experiment, we observe how a velocity profile of a shear flow gets smoothed out, whence we can determine the kinematic viscosity. In the second experiment, we try to simulate a von Karman vortex street by letting the lattice gas flow past an obstacle.

2. The pair interaction automaton

Our lattice gas model, in the case of two dimensions, is defined as follows. We use the "alternating" lattice shown in figure 1, whose node points $\vec{x} = (x_1, x_2)$ have coordinates

$$\begin{aligned} x_j \in \mathbf{Z}_e \quad &\text{if} \quad t \in \mathbf{Z}_e \\ x_j \in \mathbf{Z}_o \quad &\text{if} \quad t \in \mathbf{Z}_o \\ (j \quad &= \quad 1, 2) \end{aligned} \tag{2.1}$$

at times $t = 0, 1, 2, \ldots$, where $\mathbf{Z}_e$ and $\mathbf{Z}_o$ are the set of even and odd integral numbers, respectively. Located at each lattice point are four cells (compare figure 2), where each of the cells corresponds to one of the four possible discrete velocity vectors $\vec{v} = (v_1, v_2)$ with components

$$v_j \quad = \quad \pm 1 \qquad (j = 1, 2)$$

The state of a cell $(t, \vec{x}, \vec{v})$ is specified by three bits (n_0, n_1, n_2). The value of the bit n_0 indicates whether the cell is occupied $(n_0 = 1)$ or empty

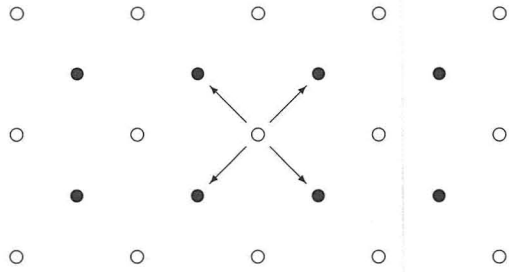

Figure 1: Lattice structure of our model. Particle positions at even and odd times are shown as white and black circles, respectively. The arrows indicate the four possible particle velocities.

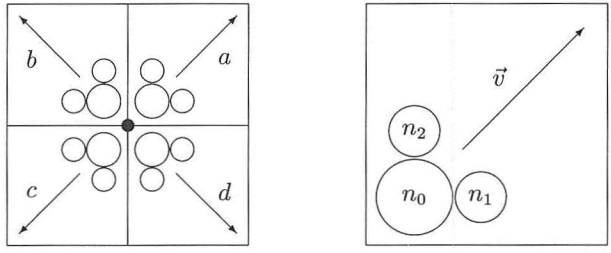

Figure 2: Attempt to illustrate the cellular structure of our model. The left picture shows all the local cells (indicated by the squares) belonging to one of the lattice points (indicated by the dot in the middle); the right picture shows one of the cells in more detail. Each circle corresponds to a bit in the computer.

($n_0 = 0$); we call n_0 the *mass* of the cell. The two remaining bits (n_1, n_2) are always zero for an empty cell, but may take arbitrary Boolean values (0 or 1) for an occupied cell. We define, in a somewhat unconventional manner, the *momentum* $\vec{m} = (m_1, m_2)$ of the cell $(t, \vec{x}, \vec{v})$ by

$$m_j(t, \vec{x}, \vec{v}) \;=\; v_j n_j(t, \vec{x}, \vec{v}) \qquad (j = 1, 2) \tag{2.2}$$

Note that our definition of "momentum" differs from the usual one: in our model, momentum $\neq$ mass $\times$ velocity; instead, a particle with velocity $\vec{v} = (v_1, v_2)$ may have a momentum of $\vec{m} = (v_1, v_2)$, $(v_1, 0)$, $(0, v_2)$, or $(0, 0)$, depending on the values of the bits n_1 and n_2, which may be viewed as internal degrees of freedom of the particle.

The *dynamics* of our model are given by

$$n_J(t + 1, \vec{x} + \vec{v}, \vec{v}) \;=\; n'_J(t, \vec{x}, \vec{v}) \qquad (J = 0, 1, 2) \tag{2.3}$$

where n_J and n'_J denote respectively the bit values immediately before and after the interactions that may take place between particles when they meet at times $t = 0, 1, 2, \ldots$ at the lattice points. Note that in equation (2.3) and elsewhere in this text, we are using uppercase and lowercase index letters to indicate different ranges of allowed values: $J \in \{0, 1, 2\}$ but $j \in \{1, 2\}$. The interactions $n_J \to n'_J$ are instantaneous and local (between the four cells at a lattice point). Equation (2.3) states that the particles move freely according to their velocity vectors $\vec{v}$ during the unit time intervals between the integer-valued instants of time.

Our interaction rule is composed of pair interactions of cells and consists of two successive steps (see figure 3):

$$n_J \;=\; n_J^1 \;\to\; n_J^2 \;\to\; n_J^3 \;=\; n'_J \tag{2.4}$$

In the first step, $n_J^1 \to n_J^2$, the interacting pairs are formed by cells whose velocity vectors differ only in the first component: $\vec{v} = (\pm 1, v_2)$ with the same value of v_2 for both partners ("horizontal pair"). In the second step, $n_J^2 \to n_J^3$, the partners differ only in the second velocity component: $\vec{v} = (v_1, \pm 1)$ with the same v_1 ("vertical pair").

Our pair interaction rules conserve the total mass and momentum of each interacting pair. For the interaction between two horizontal cells (here: cells a and b, compare figure 2) they can be derived from the following table (see also figure 4):

a_0	b_0	a_1	b_1	a'_0	b'_0	a'_1	b'_1	a'_2	b'_2
0	1	0	0	1	0	0	0	b_2	a_2
1	0	0	0	0	1	0	0	b_2	a_2
1	1	0	0	1	1	1	1	b_2	a_2
1	1	1	1	1	1	0	0	b_2	a_2
1	1	0	1	1	1	1	0	b_2	a_2
1	1	1	0	1	1	0	1	b_2	a_2

(2.5)

where a_0 and b_0 are the mass bits and a_1, a_2, b_1, and b_2 are the momentum bits of cells a and b before interaction; the bits after interaction are indicated

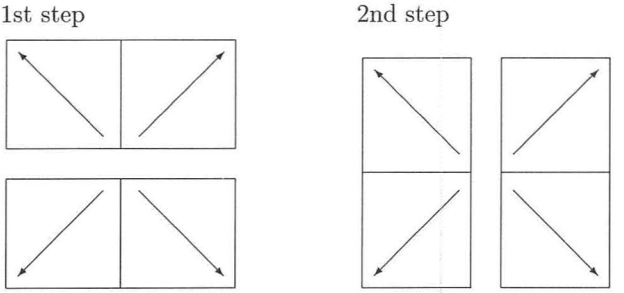

Figure 3: Subsequent formation of horizontal and vertical pairs of interacting cells in the collision process. The "process" is instantaneous (it takes no time in the model) and local (it does not involve any cells located at different lattice points). The squares represent the four local cells, and their velocity vectors are indicated by the arrows.

by an apostrophe ($'$). In cases not listed in the table, we set $a'_J = a_J$ and $b'_J = b_J$. After interaction in the horizontal direction between cells a and b and between cells c and d ($n_J^1 \to n_J^2$), the four cells will interact in the vertical direction (between cells a and c and between cells b and d) in the same manner ($n_J^2 \to n_J^3$).The dynamics of our automaton are now completely defined.

The pair-wise mass and momentum conservation follows from the properties

$$\begin{aligned} a'_0 + b'_0 &= a_0 + b_0 \\ a'_1 - b'_1 &= a_1 - b_1 \\ a'_2 + b'_2 &= a_2 + b_2 \end{aligned}$$

of table (2.5). Furthermore, we note that not only two-particle interactions (third through sixth line of the table), but also one-particle interactions (first and second line) may occur. In a one-particle interaction, the "self-colliding" particle changes its velocity while retaining its momentum. This and all the other transitions listed in (2.5) are only possible because of our unconventional definition of momentum in equation (2.2).

Since we want to simulate hydrodynamic phenomena, the observables of interest in our model are not the states of individual cells, but rather the *macroscopic* densities ρ and $\vec{q}$ of mass and momentum, respectively, given by

$$\begin{aligned} \rho(t,\vec{x}) &= \frac{1}{4}\left\langle \sum_{\vec{v}} n_0(t,\vec{x},\vec{v}) \right\rangle \\ q_j(t,\vec{x}) &= \frac{1}{4}\left\langle \sum_{\vec{v}} m_j(t,\vec{x},\vec{v}) \right\rangle = \frac{1}{4}\left\langle \sum_{\vec{v}} v_j n_j(t,\vec{x},\vec{v}) \right\rangle \\ & \qquad (j=1,2) \end{aligned}$$

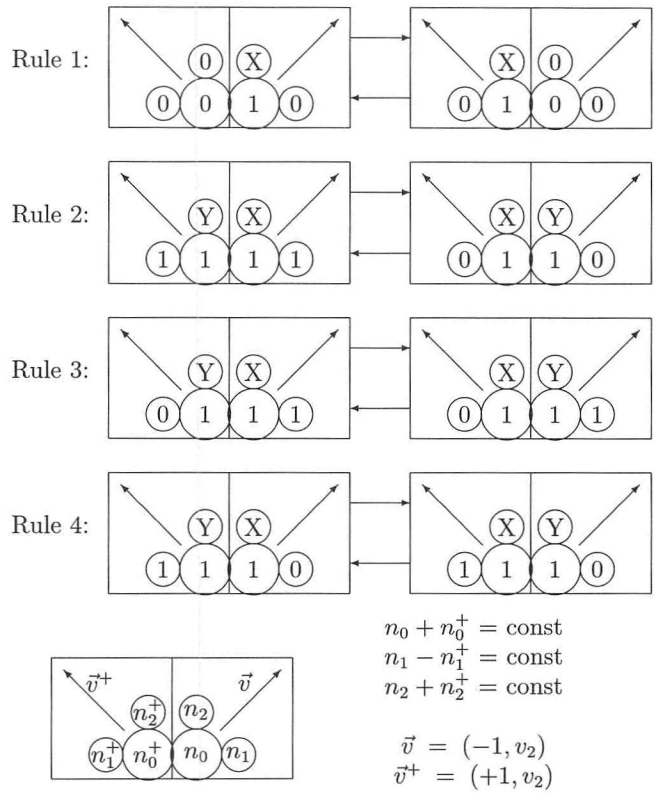

Figure 4: The pair interaction rules, illustrated for a "horizontal" interaction. A legend of the diagrams is given at the bottom, where the conservation laws are also indicated. $\vec{v}$, $\vec{v}^+$, n_J, and n_J^+ denote the velocity vectors with respect to state bits of the partner cells. When only one cell contains a particle and the other is empty, that particle can "spontaneously" change its velocity (jump to the partner cell) without changing its momentum (rule 1). When both cells are occupied by particles, these particles necessarily retain their velocities, but a transfer of momentum from one particle to the other is possible (rules 2 through 4).

where the sums extend over all four possible values of $\vec{v}$ with $v_j = \pm 1$, and the average $\langle \cdot \rangle$ is taken over many lattice points in some neighborhood of $\vec{x}$. By applying to our model the usual Gibbs formalism of statistical mechanics and then making a Chapman-Enskog type expansion, in a manner similar to that done for the conventional cellular-automaton fluids [5], one obtains the hydrodynamic equations [13]

$$\begin{aligned} \vec{\nabla} \cdot \vec{u} &= 0 \\ \frac{\partial \vec{u}}{\partial t} + (\vec{u} \cdot \vec{\nabla})\vec{u} + \vec{\nabla}\phi &= 0 \end{aligned} \tag{2.6}$$

with

$$\phi := \frac{4}{9}\rho \qquad \vec{u} := \frac{8}{9}\vec{q}$$

Equations (2.6), which have the usual form of fluid-dynamic Euler equations, are valid for the lattice gas only in the low-velocity, incompressible, nondissipative limit, for a mean mass density of $\rho = 1/2$. When these limiting conditions are not satisfied, the automaton's hydrodynamics are described by anisotropic equations whose forms are considerably more complicated than (2.6).

Unfortunately, the theoretical prediction of dissipative effects—particularly the shear viscosity, which is of great practical interest—is very difficult, and no results are available yet. We can, however, "measure" the viscosity by computer experiments.

3. Measurement of the shear viscosity

3.1 The smoothing-out of a discontinuity in velocity

A simple method to measure the shear viscosity of lattice gases has been described by Lim [10]. The initial setup consists of two adjacent streams moving at the same velocity U but in opposite directions:

$$\begin{aligned} u_1 &= \begin{cases} -U & \text{for } y < 0 \\ +U & \text{for } y > 0 \end{cases} \\ u_2 &= 0 \\ & \quad (\text{at } t = 0) \end{aligned}$$

where $\vec{u} =: (u_1, u_2)$. The analytical solution of the incompressible Navier-Stokes equations with this initial condition is known:

$$u_1 = U \operatorname{erf} \frac{y}{\sqrt{4\nu t}} \qquad v = 0$$

where erf is the error function and ν is the kinematic shear viscosity coefficient. Linearizing the error function for small values of the argument ($\ll 1$), we have

$$u_1 \approx \frac{Uy}{\sqrt{\pi \nu t}}$$

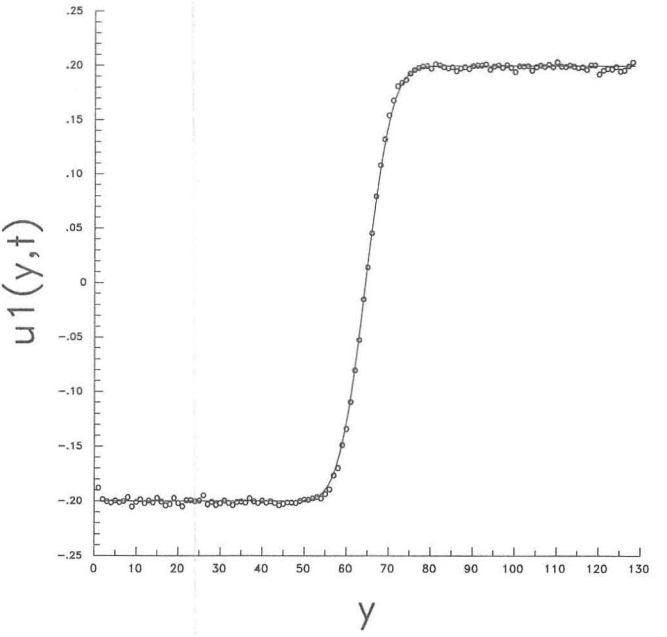

Figure 5: Measurement of the shear viscosity $\nu : u_1(y,t)$ over y (after 6000 time steps): data points (o) and fitted error function.

The viscosity can be calculated by linear regression applied to the observed velocity profile $u_1(t,y)$ for sufficiently small y at different times t. The size of our computational domain is 2048×2048 units, and we use macro-cells for coarse-graining (local averaging over $\vec{x}$) of size 64×16. The vertical velocity component v and the density deviation from $1/2$ remain small during the simulation: after $t = 6000$ timesteps we observe $u_2 = 0.000 \pm 0.014$ and $\rho = 0.500 \pm 0.015$. The x-averaged mean values $U(t,y) = \langle u_1(t,x,y) \rangle_x$ and the corresponding standard deviations are calculated from 32 macro-cell values along the x-direction. The results of the linear fit near $y = 0$ (see figure 5) are shown in the following table:

t	2000	4000	6000
ν	0.49	0.52	0.48

The value of the kinematic shear viscosity is similar to that of the FHP-2 model at the same density (FHP-1: $\nu = 1.2$; FHP-2: $\nu = 0.68$; FHP-3: $\nu = 0.075$ [5]). Only recently Rothman [15] has given (non-local) collision rules for FHP that result in even negative viscosity.

3.2 Shear wave relaxation measurements

As shown by d'Humieres and Lallemand [3], the relaxation of an initial shear wave on a square lattice with periodic boundary conditions can be used to measure the shear viscosity ν, the bulk viscosity η, and the speed of sound c. The initial perturbation consists of a longitudinal and a transversal mode and has the form

$$(\vec{u}_l + \vec{u}_t)\cos(\vec{k}\cdot\vec{r}) \tag{3.1}$$

where $\vec{u}_l$ is the longitudinal mode, $\vec{u}_t$ is the transversal mode, and $\vec{k}$ is the wave vector. By solving a linearized Navier-Stokes equation with (3.1), one gets the relaxation of the initial velocity modes and a density perturbation $\delta\rho$ coupled to the longitudinal mode [11]:

$$\begin{aligned}
\vec{u}(\vec{r},t) &= \left(\vec{u}_l\cos(\omega t)\exp\left(-\frac{k^2(\nu+\eta)}{2}t\right)\right. \\
&\qquad \left. +\vec{u}_t\exp\left(-k^2\nu t\right)\right)\cos(\vec{k}\cdot\vec{r}) \\
\delta\rho(\vec{r},t) &= \left(\frac{\rho u_l}{c}\sin(\omega t)\exp\left(-\frac{k^2(\nu+\eta)}{2}t\right)\right)\sin(\vec{k}\cdot\vec{r})
\end{aligned} \tag{3.2}$$

with $\omega = ck$ and $(k(\nu+\eta)/2\rho c)^2 \ll 1$. A typical set of the relaxation curves is shown in figure 6. To obtain the relaxation curves, the transversal and longitudinal velocities and the density have been averaged perpendicular to the wave vector at each time step. Then the interesting component of the initial wave has been extracted by a Fourier transformation as a function of time. The viscosities ν and η and the speed of sound c were calculated by least-squares fits of the above equations (3.2) to the measured relaxation curves. We performed our measurements on a lattice of 512×512 nodes with wavelengths between 64 and 128 nodes and at a density per cell of $\rho = 0.5$. We let the shear wave propagate in the x- and y-directions. This is easily attained by exchanging the succession of interacting pairs in the lattice gas. Within the uncertainty of our measurements we obtained the same values for both directions. For sufficiently small mean velocities the results are independent of wavelength and mean velocity. We have obtained $\nu = 0.46 \pm 0.02$ for the kinematic shear viscosity, which is in good agreement with the previous method. The bulk viscosity η seemed to have its value below 0.02, so we were unable to determine it. For the sound velocity c we have measured $c = 0.58 \pm 0.02$, a confirmation of the predicted theoretical value of $c = \sqrt{1/3} \approx 0.577$ for $\rho = 0.5$ of Nasilowski [13]. The results of the

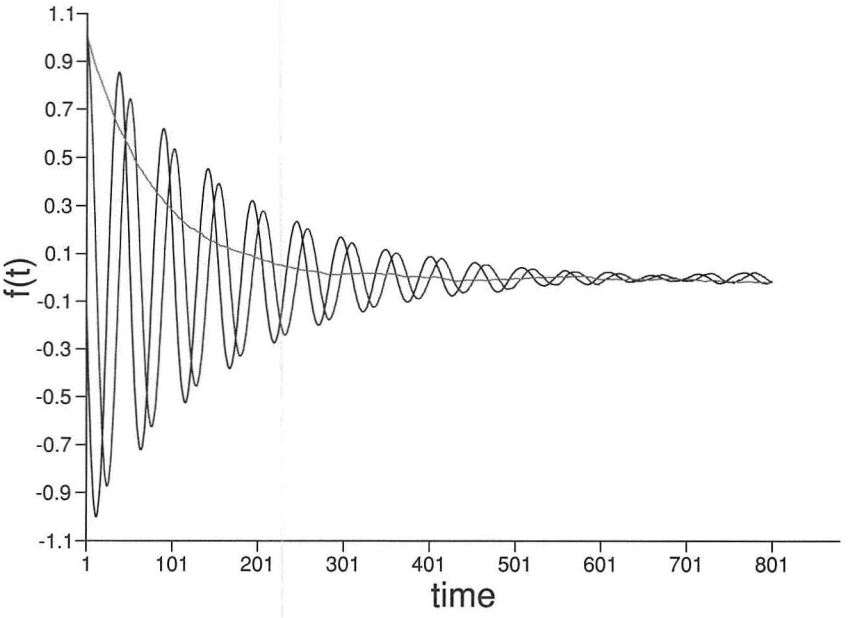

Figure 6: Shear wave relaxation measurements. A typical set of measured relaxation curves.

measurements are summarized in the following table:

u	ρ	λ	direction	ν	η	c
0.05	0.5	128	y	0.46	< 0.02	0.58
0.05	0.5	128	x	0.48	< 0.02	0.58
0.07	0.5	128	y	0.46	< 0.02	0.58
0.07	0.5	128	x	0.46	< 0.02	0.58
0.05	0.5	64	y	0.47	< 0.02	0.59
0.10	0.5	64	y	0.46	< 0.02	0.58

4. Von Karman vortex street

In the literature, the von Karman vortex street serves as a classical example for the complexity of flow patterns that may occur in systems governed by the Navier-Stokes equations from a phenomenological point of view [8]. We performed the vortex street simulations on a domain of size 6400×3200, with periodic boundary conditions in the x-direction and free slip at the y-boundaries. The width of the obstacle is 400 units. With a speed of $u = 0.1$ and a kinematic shear viscosity of 0.5, one gets a Reynolds number of 80. Figure 7 shows the flow pattern at $t = 80{,}000$.

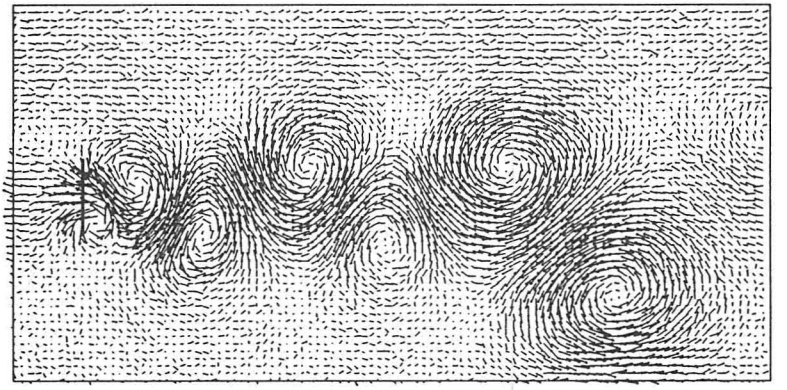

Figure 7: Von Karman vortex street. The flow pattern after 80,000 time steps (the mean flow has been subtracted) on a lattice of 6400×3200 nodes with a velocity of $u = 0.1$. With an obstacle of length 400 nodes the Reynolds number is 80.

5. Conclusions

Our simulations show that the new cellular-automaton model indeed shows the expected fluid-dynamical behavior. Moreover, we have obtained by measurement a numerical value of the shear viscosity coefficient and the sound speed. Whether dissipative effects are (at least approximately) isotropic in our lattice gas is still an open question.

Acknowledgment

We are grateful to Mr. Charilaos Kougias for teaching us important programming techniques for lattice gas automata. Publication No. 417 of the Alfred Wegener Institute for Polar and Marine Research.

References

[1] D. Burgess, F. Hayot, and W. F. Saam, "Model for Surface Tension in Lattice-Gas Hydrodynamics," *Physical Review A*, **38**(7) (1988) 3589–3592.

[2] P. Clavin, P. Lallemand, Y. Pomeau, and G. Searby, "Simulation of Free Boundaries in Flow Systems by Lattice-Gas Models," *Journal of Fluid Mechanics*, **188** (1988) 437–464.

[3] D. d'Humières and P. Lallemand, "Lattice Gas Automata for Fluid Mechanics," *Physica*, **140A** (1986) 326–335.

[4] U. Frisch, B. Hasslacher, and Y. Pomeau, "Lattice-Gas Automata for Navier-Stokes Equations," *Physical Review Letters*, **56** (1986) 1505.

[5] U. Frisch, D. d'Humières, B. Hasslacher, P. Lallemand, Y. Pomeau, and J.-P. Rivet, "Lattice Gas Hydrodynamics in Two and Three Dimensions," *Complex Systems*, **1** (1987) 649–707.

[6] J. Hardy, O. de Pazzis, and Y. Pomeau, "Molecular Dynamics of a Classical Lattice Gas: Transport Properties and Time Correlation Functions," *Physical Review A*, **13** (1976) 1949.

[7] M. Henon, "Isometric Collision Rules for the Four-Dimensional FCHC Lattice Gas," *Complex Systems*, **1** (1987) 475–494.

[8] L. P. Kadanoff, "On Two Levels," *Physics Today*, **39**(9) (1986) 7–9.

[9] A. J. C. Ladd and M. E. Colvin, "Application of Lattice-Gas Cellular Automata to the Brownian Motion of Solids in Suspension," *Physical Review Letters*, **60**(11) (1988) 975–978.

[10] H. A. Lim, "Lattice Gas Automata of Fluid Dynamics for Unsteady Flow," *Complex Systems*, **2** (1988) 45–58.

[11] R. D. Mountain, "Spectral Distribution of Scattered Light in a Simple Fluid," *Reviews of Modern Physics*, **38**(1) (1966) 205–214.

[12] R. Nasilowski, "An Arbitrary-Dimensional Cellular-Automaton Fluid Model with Simple Rules," to appear in *Proceedings in Dissipative Structures in Transport Processes and Combustion*, Interdisciplinary Seminar, Bielefeld (Springer-Verlag, Heidelberg, 1989).

[13] R. Nasilowski, "A Cellular-Automaton Fluid Model with Simple Rules in Arbitrarily Many Dimensions," submitted to *Journal of Statistical Physics*.

[14] D. H. Rothman, "Cellular-Automaton Fluids: A Model for Flow in Porous Media," *Geophysics*, **53**(4) (1988) 509–518.

[15] D. H. Rothman, "Negative-Viscosity Lattice Gases," *Journal of Statistical Physics*, **56**(3/4) (1989) 517–524.

[16] D. H. Rothman and J. M. Keller, "Immiscible Cellular-Automaton Fluids, *Journal of Statistical Physics*, **52** (1988) 1119–1127.

[17] S. Succi, P. Santangelo, and R. Benzi, "High Resolution Lattice Gas Simulation of Two-Dimensional Turbulence," *Physical Review Letters*, **60** (1988) 2738–2740.